

Effective nonadditive pair potential for lock-and-key interacting particles: The role of the limited valence

Julio Largo,¹ Piero Tartaglia,² and Francesco Sciortino¹

¹Dipartimento di Fisica and INFM-CNR-SOFT, Università di Roma La Sapienza, Piazzale A. Moro 2, 00185 Roma, Italy

²Dipartimento di Fisica and INFM-CNR-SMC, Università di Roma La Sapienza, Piazzale A. Moro 2, 00185 Roma, Italy

(Received 15 March 2007; published 13 July 2007)

Theoretical studies of self-assembly processes and condensed phases in colloidal systems are often based on effective interparticle potentials. Here we show that developing an effective potential for particles interacting with a limited number of “lock-and-key” selective bonds (due to the specificity of biomolecular interactions) requires—in addition to the nonsphericity of the potential—a (many body) constraint that prevents multiple bonding on the same site. We show the importance of retaining both valence and bond selectivity by developing, as a case study, a simple effective potential describing the interaction between colloidal particles coated by four single-strand DNA chains.

DOI: 10.1103/PhysRevE.76.011402

PACS number(s): 82.70.Dd, 61.20.Gy, 61.20.Ja

Description of multiscale phenomena in self-assembling systems and understanding of their collective behavior requires a coarse graining process in which the irrelevant degrees of freedom are integrated out in favor of an effective renormalized interaction potential [1]. Colloidal systems are often described by this type of approach, in which the solvent and its chemical-physical properties are encoded into parameters of the resulting effective inter-colloid particle potential [2]. Thermodynamic (and often also dynamic) bulk behavior of several complex particles, including polymers, star polymers, dendrimers, micelles, telechelic polymers [3–8] has been interpreted on the basis of effective pairwise potentials, function only of the distance between particle centers.

Very recently, design of new materials has started to capitalize on the possibilities offered by complementary “lock-and-key” selective interactions [9], aiming to achieve a much better control on the resulting bonding pattern and on the mechanical properties of the self-assembled bulk material. In this work we show that effective potentials for these new particles must account for both the valence (maximum number of bonds) and for the selectivity of the bonding process. While at the microscopic level specificity in the bonding interactions is pairwise additive—it builds on steric incompatibilities [10], e.g., on excluded volume effects which prevent the possibility of multiple interactions at the same bonding site—we find that the conservation of this important feature at the level of the coarse-grained effective potential may require the breakdown of the pairwise additive approximation.

As a working example, we discuss the development of an effective potential for a macromolecule composed by a core particle decorated by a small number of short single strands (ss) DNA [11] to show (i) the importance of properly accounting for valence and bond selectivity; (ii) the need for a nonpairwise additive effective potential. The full model is graphically explained in Fig. 1 (and the chosen length and energy units), and more in detail Refs. [12,13]. A semirigid chain of eight particles, modeling a 8-base ss-DNA, is attached to each of the four particles composing a central tetrahedral core. Each of the 32 base particles carries an addi-

tional interaction site (labeled A,T,G, or C) which can bind only with complementary site types (only A-T or G-C binding are allowed), resulting in a total of 68 interaction sites per macromolecule. The chosen base sequence is palindromic, so that all eight bases can be simultaneously paired when ss-DNA arms of different macromolecules approach in the correct orientation. All site-site interactions are pairwise additive. The phase diagram of this model shows a region of

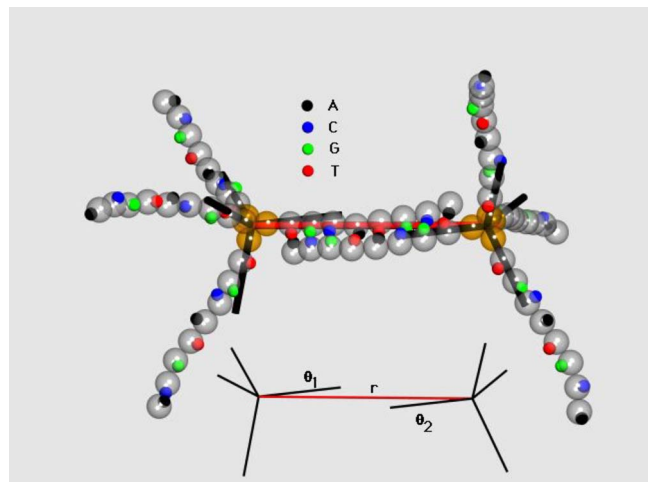


FIG. 1. (Color online) Drawing of two macromolecules in a bonded configuration. Each macromolecule is composed by a tetrahedral hub (four tetrahedrally-oriented orange spheres) to which four single strands of eight bases each (large spheres) are anchored. Each base is decorated by a short-range attractive site (small spheres) encoding the base type (A,T,G,C). Base complementary is enforced by selective attractive interactions between A and T and between G and C sites. In the process of developing a coarse-grained model, we associate a rigid tetrahedron (oriented according to the central core of the particle) to each macromolecule and focus on the center-to-center distance r and on the two angles θ_1 and θ_2 , defined in the figure. We use as unit of length the diameter of the larger spheres and as a unit of energy the A-T (or the equivalent G-C) binding energy. Number density is defined as the total number of large spheres (36 for each macromolecule) divided by the volume.

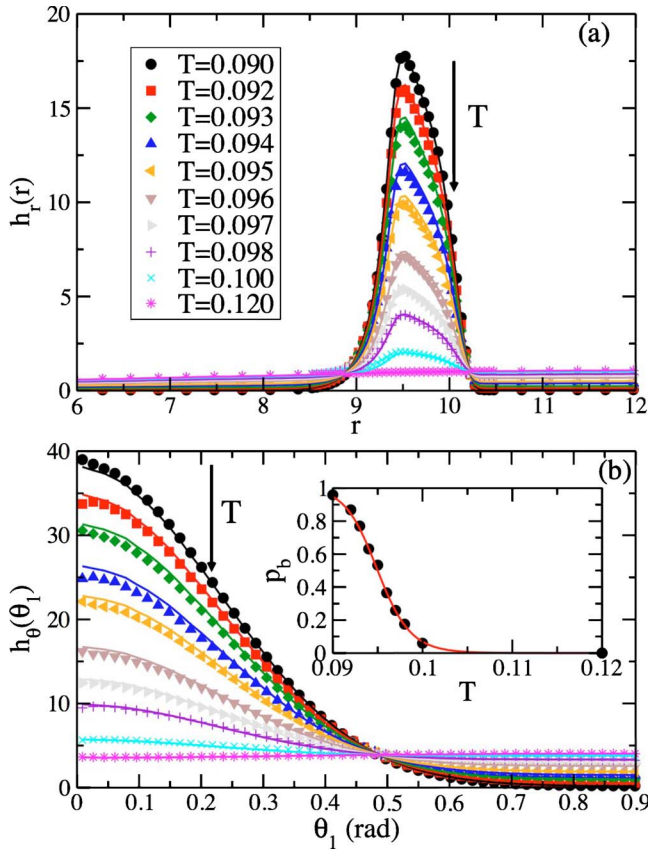


FIG. 2. (Color online) Results from the simulation of two macromolecules in a box of side $L=25$: center-to-center probability $h_r(r)$ (a) and angle θ_1 distribution $h_\theta(\theta_1)$ [$h_\theta(\theta_2)=h_\theta(\theta_1)$ for symmetry] (b). Symbols are numerical results for different T . Lines are the corresponding expressions provided by Eq. (2) after integration over θ_1 and θ_2 in panel (a) or integration over r and θ_2 in panel (b). The inset shows the T dependence of p_b and its fit to a two-state model (see text) with $\Delta E=4.94$ and $\Delta S/k_B=52$ (k_B is the Boltzmann constant).

gas-liquid phase separation, but only at small number densities ρ . The liquid region is characterized by the presence of a four-coordinated network, whose dynamics progressively slows down on cooling, parallel to the formation of an open gel-like structure [13].

To evaluate the effective potential we simulate, using Monte Carlo methods, a system composed of two macromolecules in a box for several temperatures T , covering the T region where ss-DNA pairs. From a large ensemble of equilibrium configurations we extract the properties of the degrees of freedom to be retained in the coarse-grained model: (i) the normalized probability h_r of finding the two particles at relative center-to-center distance r (i.e., in such a way that $\frac{1}{L^3} \int 4\pi h_r r^2 dr = 1$) and (ii) the normalized probabilities h_{θ_1} and h_{θ_2} of the angle θ_1 and θ_2 between \vec{r} and the closest ss-DNA arm on each particle (so that $\frac{1}{2} \int_0^\pi h_\theta \sin \theta d\theta = 1$). The variables r , θ_1 , and θ_2 are defined in Fig. 1. The T dependence of $h_r(r)$ and $h_\theta(\theta_1)$ is shown in Fig. 2. On cooling, angular and spatial correlations build up, reflecting the formation of a stable double-strand configuration, with a char-

acteristic center-to-center distance of the order of the DNA arm length ($8.5 \leq r \leq 10.5$) and a preferential orientation for linear bonding ($\theta_1 \approx 0$). At the highest and lowest investigated T , h_r and h_θ describe, to a good approximation, the fully nonbonded (nb) and fully bonded (b) state, respectively. The nonbonded high T state is characterized by essentially unstructured h_θ^{nb} and h_r^{nb} , except for the r region close to the origin where excluded volume interactions play a role. The function h_r^b is well described by a Gaussian distribution $h_r^b = \frac{A}{\sqrt{2\pi\sigma^2}} e^{-\theta^2/2\sigma^2}$ (where the normalization constant is $A=22.32$ and the best fit $\sigma^2=0.052 \text{ rad}^2$). A similar angular distribution has been recently chosen to model self-assembly of patchy particle [14]. The distribution h_θ^b is essentially localized only between $8.5 \leq r \leq 10.5$, corresponding to the bonded distance. We have not been able to provide a simple analytic best-fit expression for h_r^b and h_θ^b and, in the following, we have used their numerical values. The sharp separation in configuration space between the bonded and the nonbonded states (due to the localized nature of the interaction and to its specificity) suggests to describe the distributions at intermediate T as a linear combination of the b and nb distributions, weighted, respectively, by the probability of being bonded [$p_b(T)$] or nonbonded [$1-p_b(T)$]. Lines in Fig. 2 show that both h_r and h_θ can indeed be described as linear combinations [with the same $p_b(T)$ coefficient] of the b and nb distributions. Moreover, as shown in the inset of Fig. 2, the resulting T dependence of $p_b(T)$ is very well fitted by the two-state expected theoretical expression $p_b(T)=1/(1+e^{-(\Delta U-T\Delta S)/k_B T})$, where ΔU and ΔS measure the change in energy and entropy associated to the formation of a double strand. The important result is that the T dependence decouples from the r and θ dependence and it becomes possible to write the probability of finding the two macromolecules at relative distance r and angles θ_1 and θ_2 as

$$P(r, \theta_1, \theta_2, T) = p_b(T) P^b(r, \theta_1, \theta_2) + [1 - p_b(T)] P^{nb}(r, \theta_1, \theta_2). \quad (1)$$

We approximate $P^b(r, \theta_1, \theta_2) = h_r^b(r) h_\theta^b(\theta_1) h_\theta^b(\theta_2)$ and analogously P^{nb} for the nonbonded case. In this approximation, correlation between distances and angles within the b (or the nb) state are neglected, since both P^b and P^{nb} are written as a product of their arguments. We have tested that this is indeed a good approximation. Correlation between angles and distances arising from the differences between b and nb states (small θ_1 and θ_2 are found when r is within the bonding distance) are retained in P , which indeed cannot be factorized.

Thus the four functions h_r^b , h_θ^b , h_r^{nb} , h_θ^{nb} , and $p_b(T)$ fully specify $P(r, \theta_1, \theta_2, T)$. It is thus possible to model the macromolecule as a particle decorated by four tetrahedrally oriented arms and evaluate an effective potential between these particles. The simplest approach is to neglect the angular correlation and develop a spherical (s) effective potential $V_s(r, T)$, integrating out the angular degrees of freedom as

$$\beta V_s(r, T) = -\ln \frac{p_b(T) h_r^b(r) + [1 - p_b(T)] h_r^{nb}(r)}{p_b(T) h_r^b(r_\infty) + [1 - p_b(T)] h_r^{nb}(r_\infty)}. \quad (2)$$

Here r_∞ is any distance larger than the range of interaction of the two molecules [so that $V_s(r, T)=0$ at large distances]. A

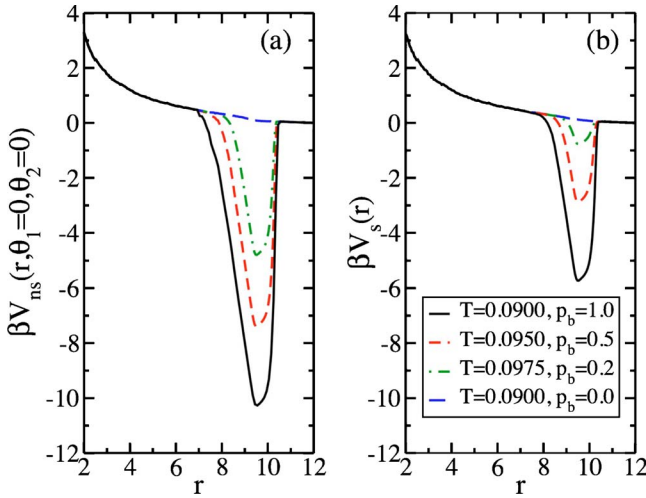


FIG. 3. (Color online) (a) Shape of the nonspherical effective potential $\beta V_{ns}(r)$ for given angles $\theta_1=0$ and $\theta_2=0$, and (b) the spherically averaged effective potential $\beta V_s(r)$, for different temperatures.

more accurate approach requires retaining information on the angular orientations, defining a nonspherical (ns) angular dependent potential V_{ns} as

$$\beta V_{ns}(r, \theta_1, \theta_2, T) = -\ln \frac{P(r, \theta_1, \theta_2, T)}{P(r_\infty, \theta_1, \theta_2, T)}. \quad (3)$$

By construction, both V_s and V_{ns} accurately describe the radial distribution function (and, in the case of V_{ns} , also the

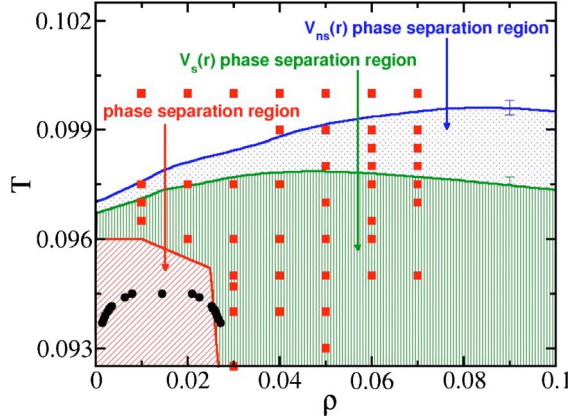


FIG. 4. (Color online) Phase diagram of the model for colloidal particles coated by four single-strand DNA chains. The area labeled as phase separation region approximately indicates the region where phase separation is expected for the model studied in Ref. [13] (estimates based on the extrapolated behavior of the low wave-vector structure factor). Filled squares, denote the stable state points studied in Ref. [13]. The graph also shows the boundary between homogeneous and phase-separated states for V_s and V_{ns} . Note that most of the filled squares are located in a region of the phase diagram where phase separation is observed in V_s or V_{ns} . The filled circles indicate the gas-liquid coexistence for the valency constrained effective model.

angular distribution function) of the system in the limit of vanishing density at all T . The radial shape of the two resulting potentials is shown in Fig. 3, V_{ns} has a deeper minimum than V_s , to compensate for the reduction of the solid angle associated to bonding.

To assess the ability of the two potentials in reproducing the bulk behavior of the original model and to estimate the importance of the directional interactions, we compare the phase diagram of the two potentials, with the (previously studied) behavior of the original model [12,13]. Both V_s and V_{ns} perform very badly, predicting a very wide region of liquid-gas instability, which includes the region where the tetrahedral network of bonded particles is known to be the stable phase (see Fig. 4). The unstable gas-liquid region is even wider in the case of V_{ns} , due to its deeper minimum. The disagreement is so large that no state points can be chosen to compare the original and the effective models in the region where a network develops, since V_s and V_{ns} always generate a phase-separated configuration.

The failure in reproducing the bulk behavior can be ascribed to the absence, in both V_s and V_{ns} , of the lock-and-key character of the interaction. In the real model, once a ss-DNA is linked to a complementary strand of a different particles, it is not available for further bonding. The specificity of the interaction implies that each ss-DNA cannot be simultaneously bonded to more than one other arm. This important rule is not enforced neither by V_s (which allows for a large number of bonded neighbors) nor by V_{ns} since the width of

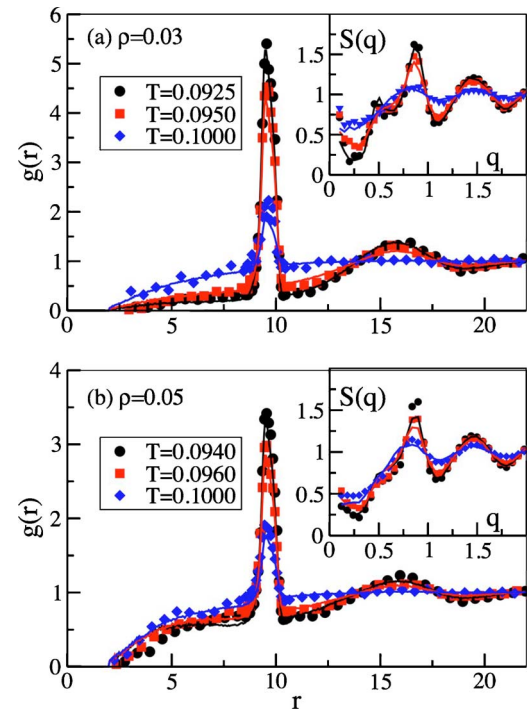


FIG. 5. (Color online) Radial distribution functions $g(r)$ for the original model (points, from Ref. [13]) and the valency-constrained effective potential (lines) at $\rho=0.03$ (a) and $\rho=0.05$ (b). Inset: structure factors $S(q)$ at the same state points. Note the increase in $S(q)$ at small q when $\rho=0.03$, signaling the proximity of the limit of stability of the liquid phase.

the angular part of V_{ns} does not prevent multiple bonding at the same arm direction. We are forced to abandon the pairwise additivity approximation and develop a new potential which enforces the bond selectivity and the valence (so that each particle cannot be engaged in more than four bonds). To this aim, we complement V_{ns} with an *ad hoc* rule imposing that each arm can be engaged only in one bond, very much in the same spirit as the maximum valence models [15]. From a computational point of view, during the simulation, we retain a list of all pairs of bonded arms and make sure that each arm is involved at most in one bonded interaction. The resulting effective valency-constrained nonspherical model is able to generate homogeneous equilibrium states in the expected region of the phase diagram. This opens the possibility to compare the predictions of the effective model with those of the original model [13], at the same T and ρ . A comparison in real and in reciprocal space is shown in Fig. 5. The limited-valence effective model is able to reproduce with satisfactory accuracy the structure of the tetrahedral network: both the peculiar ratio between the position of the first and second peak in the center-center radial distribution function $g(r)$ as well as the development of a pre-peak in the corresponding structure factor $S(q)$ on cooling are well captured by the effective potential. To locate precisely the gas-liquid coexistence for the limited-valence effective potential we perform

umbrella sampling grand canonical Monte Carlo simulations [16] (and histogram reweighting techniques [17]). The resulting gas-liquid coexistence curve is shown in Fig. 4. As compared to the unconstrained V_s and V_{ns} , the region of gas-liquid instability is now confined to small ρ , opening up a window of densities (above the liquid coexistence branch) in which equilibrium liquid states can be accessed.

In summary, we have shown that in the process of developing effective potentials for particles with low valence and with selective interactions (as in functionalized colloids) it is mandatory to account for the specificity of the interaction which intrinsically limit the maximum number of bonds that can be formed. The present study shows that colloidal particles with specific interactions constitute another class of colloidal systems for which pair additivity approximation breaks down in the effective potential, in addition to the recently reported case of charge-stabilized colloidal crystal [18]. The importance of retaining, in addition to the directionality, the valence of the original model is clearly evidenced by the fact that valence strongly controls the width of the gas-liquid coexistence [19,20].

We thank C. Likos, F. W. Starr, and E. Zaccarelli for valuable discussions. We acknowledge support from Miur PRIN and Grant No. MRTN-CT-2003-504712.

-
- [1] C. N. Likos, Phys. Rep. **348**, 267 (2001).
 - [2] W. B. Russel, D. A. Saville, and W. R. Schowalter, *Colloidal Dispersions* (Cambridge University Press, 1992).
 - [3] A. A. Louis, P. G. Bolhuis, J. P. Hansen, and E. J. Meijer, Phys. Rev. Lett. **85**, 2522 (2000).
 - [4] C. N. Likos, H. Löwen, M. Watzlawek, B. Abbas, O. Jucknischke, J. Allgaier, and D. Richter, Phys. Rev. Lett. **80**, 4450 (1998).
 - [5] M. Bouaskarne, S. Amokrane, and C. Regnaut, J. Chem. Phys. **114**, 2442 (2001).
 - [6] F. Lo Verso, C. N. Likos, C. Mayer, and H. Löwen, Phys. Rev. Lett. **96**, 187802 (2006).
 - [7] C. Pierleoni, C. Addison, J.-P. Hansen, and V. Krakoviack, Phys. Rev. Lett. **96**, 128302 (2006).
 - [8] M. Laurati, J. Stellbrink, R. Lund, L. Willner, D. Richter, and E. Zaccarelli, Phys. Rev. Lett. **94**, 195504 (2005).
 - [9] C. M. Niemeyer, Angew. Chem., Int. Ed. **40**, 4128 (2001).
 - [10] M. Wertheim, J. Stat. Phys. **35**, 19 (1984).
 - [11] K. Stewart and L. McLaughlin, J. Am. Chem. Soc. **126**, 2050 (2004).
 - [12] F. W. Starr and F. Sciortino, J. Phys.: Condens. Matter **18**, L347 (2006).
 - [13] J. Largo, F. W. Starr, and F. Sciortino, Langmuir **23**, 5896 (2007).
 - [14] A. W. Wilber *et al.*, e-print arXiv:cond-mat/0606634.
 - [15] R. J. Speedy and P. G. Debenedetti, Mol. Phys. **81**, 237 (1994).
 - [16] D. Frenkel and B. Smit, *Understanding Molecular Simulations* (Academic Press, San Diego, 2002).
 - [17] N. B. Wilding, J. Phys.: Condens. Matter **9**, 585 (1996).
 - [18] D. Reinke, H. Stark, H.-H. von Grünberg, A. B. Schofield, G. Maret, and U. Gasser, Phys. Rev. Lett. **98**, 038301 (2007).
 - [19] E. Zaccarelli, S. V. Buldyrev, E. La Nave, A. J. Moreno, I. Saika-Voivod, F. Sciortino, and P. Tartaglia, Phys. Rev. Lett. **94**, 218301 (2005).
 - [20] E. Bianchi, J. Largo, P. Tartaglia, E. Zaccarelli, and F. Sciortino, Phys. Rev. Lett. **97**, 168301 (2006).